EARTHQUAKE ENGINEERING AND STRUCTURAL DYNAMICS
*Earthquake Engng Struct. Dyn.* 2000; **29**:297–313

# Dynamic analysis of sliding structures with unsynchronized support motions

Yen-Po Wang* and Wei-Hsin Liao

*Department of Civil Engineering, National Chiao-Tung University, Hsinchu, Taiwan*

## SUMMARY

The dynamic analysis of sliding structures is complicated due to the presence of friction. Synchronization of the kinematics of all the isolation bearings is often granted to simplify the task. This, however, may lead to inaccurate prediction of the structural responses under certain circumstances. Stepped structures or continuous bridges with seismic isolation are notable examples where unsynchronized bearing motions are expected. In this paper, a logically simple and numerically efficient procedure is proposed to solve the dynamic problem of sliding systems with unsynchronized support motions. The motion equations for the sliding and non-sliding modes of the isolated structure are unified into a single equation that is represented as a difference equation in a discrete-time state-space form and the base shear forces between the sliding interfaces can be determined through simple matrix algebraic analysis. The responses of the sliding structure can be obtained recursively from the discrete-time version of the motion equation with constant integration time step even during the transitions between the non-sliding and sliding phases. Therefore, both accuracy and efficiency in the dynamic analysis of the highly non-linear system can be enhanced to a large extent. Rigorous assessment of seismic structures with unsynchronized support motions has been carried out for both a stepped structure and a continuous bridge. Effectiveness of friction pendulum bearings for earthquake protection of such structures has been verified. Moreover, evident unsynchronized sliding motions of the friction bearings have been observed, confirming the necessity to deal with each of the bearings independently in the analytical model. Copyright © 2000 John Wiley & Sons, Ltd.

KEY WORDS: seismic isolation; friction pendulum bearing; sliding systems

## INTRODUCTION

Seismic isolation is one of the possible solutions for civil engineering structures to sustain severe earthquakes without damage. Because of the high lateral flexibility of the isolation bearings, the vibration period of the isolated structure is lengthened so that dynamic resonance of the isolated

* Correspondence to: Yen-Po Wang, Department of Civil Engineering, National Chiao-Tung University, 1001 Ta Hsueh Road, Hsinchu, Taiwan.

Contract/grant sponsor: National Science Council of the Republic of China; contract/grant number: NSC 87-2621-P-009-002.



*Received 7 April 1999*
*Accepted 20 August 1999*

structure with the earthquakes is avoided. The isolated structure is prevented from over-displacing by further introducing high damping material to the bearings. Seismic isolation has become a reality in engineering practice since the advent of lead rubber bearings (LRB) in the early 1980s. Actually, multifarious isolation devices have been developed ever since, among which the sliding-type bearing is one of the most competitive to the rubber-type bearing. With the implementation of the sliding bearings, the base shear force transmitted to the superstructure is limited to the maximum frictional force of the sliding bearings, regardless of the severity of earthquakes. If the sliding bearings are frictionless, the transmission path of seismic forces will be completely released but excessive displacement will be restive. Fortunately, the problem of excessive displacement is relieved by the friction mechanism of the sliding bearings where vibration energy is dissipated. Moreover, with the introduction of concave sliding surfaces, restoring capability of the isolated structure can be provided through the pendulum dynamics which, in turn, changes the fundamental period of the structure and makes the friction pendulum bearings (FPB) functionally comparable to rubber bearings. Although rubber bearings have been extensively applied for base isolation, the friction pendulum bearings have found more and more applications in recent years for economic reasons [1–6].

Because non-sliding and sliding phases exist alternatively in the motion of sliding structures depending on the magnitude of the shear forces at the frictional sliding interfaces, the dynamics of sliding structures is a highly non-linear problem. The non-linear problem is so complicated that analytical solution is limited to the harmonic motions of sliding structures with no more than two degrees of freedom under idealized conditions [7–8], and more realistic transient responses of sliding structures with multiple degrees of freedom (MDOF) can only be obtained numerically. Mostaghel and Tanbakuchi [9] proposed a semi-analytical solution procedure by alternatively using two sets equations of motions, corresponding to the non-sliding and sliding phases. Yang *et al.* [10], Lu and Yang [11] proposed a numerical solution procedure by introducing a fictitious spring to the foundation floor to represent the frictional effect of the sliding bearings. In all the aforementioned studies, the sliding bearings were applied to structures erected on contour foundations where behaviors of all the isolation bearings were presumably identical. This assumption, however, may not be adequate under certain circumstances. A notable exception is the application of isolation bearings to structures with a stepped foundation where, due to structural asymmetry in elevation, unsynchronized bearing motions would occur. This makes the dynamic analysis of the isolated stepped structures even more complicated, and the existing numerical schemes cannot be adopted directly [9–11]. Recently, Wang *et al.* [12] proposed for the dynamic analysis of isolated bridge structures with unsychronized bearing motions a numerical procedure based on equilibrium and kinematics of the sliding bearings, following a prescribed friction mechanism. A unified governing equation was considered for both the sliding and non-sliding phases without changing any system parameters. Although conceptually simple, the numerical procedure was yet unwieldy because the determination of the bearing shears required an iterative process based on a corrective-pseudo-force concept.

In this paper, the dynamic problem of highly non-linear systems with unsynchronized support motions is tackled by introducing a logically simple and numerically efficient procedure. The motion equations for the sliding and non-sliding modes of the isolated structure are unified into a single equation that is represented as a difference equation in a discrete-time state-space form and the base shear forces between the sliding interfaces can be determined through matrix algebraic analysis. In the non-sliding phase, the shear force between the sliding interfaces fails to overcome the maximum frictional force of the sliding bearing. The sliding bearing remains still

 

and the relative velocity between the sliding interfaces is known to be zero, though the quantity of the frictional force is not known yet. In the sliding phase, the shear force between the sliding interfaces is large enough to overcome the maximum frictional force. The isolated bearing slides and the frictional force are known to be the maximum frictional force but the relative velocity between sliding interfaces is not known yet. Since one of the quantity, either the frictional force or the relative velocity, is known, the motion equation in the form of difference equation can be solved recursively in such a way that the integration interval remains constant throughout the whole process of dynamic analysis. Rigorous assessment of seismic structures with unsynchronized support motions has been carried out for both a stepped structure and a continuous bridge. Effectiveness of friction pendulum bearings for earthquake protection of such structures has been verified.

## SOLUTION ALGORITHM FOR GENERIC SLIDING SYSTEMS

The equation of motion of a generic sliding structure under external disturbances $\mathbf{w}(t)$ can be represented as

$$\mathbf{M}\ddot{\mathbf{u}}(t) + \mathbf{C}\dot{\mathbf{u}}(t) + \mathbf{K}\mathbf{u}(t) = \mathbf{E}\mathbf{w}(t) + \mathbf{B}\mathbf{F}(t) \tag{1}$$

where $\mathbf{u}(t)$ is the $n \times 1$ displacement vector, $\mathbf{M}$, $\mathbf{C}$, $\mathbf{K}$ are respectively, the $n \times n$ mass, damping and stiffness matrices, $\mathbf{E}$ is the $n \times q$ location matrix of the external loads, $\mathbf{w}(t)$ is the $q \times 1$ loading vector, $\mathbf{B}$ is the $n \times r$ location matrix of the friction forces and $\mathbf{F}(t)$ is the $r \times 1$ friction force vector.

*State-space representation*

Equation (1) can be represented in a state-space form, leading to a first-order differential equation as

$$\dot{\mathbf{z}}(t) = \mathbf{A}^* \mathbf{z}(t) + \mathbf{E}^* \mathbf{w}(t) + \mathbf{B}^* \mathbf{F}(t) \tag{2}$$

where

$$\mathbf{z}(t) = \begin{bmatrix} \mathbf{u}(t) \\ \dot{\mathbf{u}}(t) \end{bmatrix} \text{ is the } 2n \times \text{state vector,}$$

$$\mathbf{A}^* = \begin{bmatrix} \mathbf{0} & \mathbf{I} \\ -\mathbf{M}^{-1}\mathbf{K} & -\mathbf{M}^{-1}\mathbf{C} \end{bmatrix} \text{ is the } 2n \times 2n \text{ system matrix,}$$

$$\mathbf{B}^* = \begin{bmatrix} \mathbf{0} \\ \mathbf{M}^{-1}\mathbf{B} \end{bmatrix} \text{ is the } 2n \times r \text{ friction loading matrix, and}$$

$$\mathbf{E}^* = \begin{bmatrix} \mathbf{0} \\ \mathbf{M}^{-1}\mathbf{E} \end{bmatrix} \text{ is the } 2n \times q \text{ external loading matrix.}$$

*Discrete-time solution*

A closed-form solution of the time-invariant dynamic system (2) can be obtained as

$$\mathbf{z}(t) = \mathrm{e}^{\mathbf{A}^*(t-t_0)}\mathbf{z}(t_0) + \int_{t_0}^{t} \mathrm{e}^{\mathbf{A}^*(t-\tau)}[\mathbf{B}^*\mathbf{F}(\tau) + \mathbf{E}^*\mathbf{w}(\tau)]\,\mathrm{d}\tau \tag{3}$$

 

In order to carry out the integration involved in Equation (3), the continuous-time evolutions of $\mathbf{w}(\tau)$ and $\mathbf{F}(\tau)$ within the sampling interval are required. Since the recorded load functions are commonly discretized and the friction forces are piece-wise linear in nature, it is logical to assume linear variations of these loading functions between two consecutive sampling instants. That is

$$\mathbf{F}(\tau) = \frac{k\Delta t - \tau}{\Delta t}\,\mathbf{F}[(k-1)\,\Delta t] + \frac{\tau - (k-1)\,\Delta t}{\Delta t}\,\mathbf{F}[k\,\Delta t], \quad (k-1)\,\Delta t \leqslant \tau \leqslant k\,\Delta t \tag{4a}$$

$$\mathbf{w}(\tau) = \frac{k\Delta t - \tau}{\Delta t}\,\mathbf{w}[(k-1)\,\Delta t] + \frac{\tau - (k-1)\,\Delta t}{\Delta t}\,\mathbf{w}[k\,\Delta t], \quad (k-1)\,\Delta t \leqslant \tau \leqslant k\,\Delta t \tag{4b}$$

When $t_0 = (k-1)\,\Delta t$, $t = k\,\Delta t$, and $\mathbf{z}[k] = \mathbf{z}(k\,\Delta t)$, $\mathbf{F}[k] = \mathbf{F}(k\,\Delta t)$, etc. are assigned, from Equation (3), the analytical solution to the state Equation (2) is a difference equation as

$$\mathbf{z}[k] = \mathbf{A}\mathbf{z}[k-1] + \mathbf{B}_0\mathbf{F}[k-1] + \mathbf{B}_1\mathbf{F}[k] + \mathbf{E}_0\mathbf{w}[k-1] + \mathbf{E}_1\mathbf{w}[k] \tag{5}$$

where $\mathbf{A} = \mathrm{e}^{\mathbf{A}^*\Delta t}$ is the $2n \times 2n$ discrete-time system matrix, $\mathbf{B}_0 = [(\mathbf{A}^*)^{-1}\,\mathbf{A} + (1/\Delta t)(\mathbf{A}^*)^{-2}\,(\mathbf{I} - \mathbf{A})]\,\mathbf{B}^*$ is the $2n \times r$ discrete-time friction loading matrix of the previous time step, $\mathbf{B}_1 = [-(\mathbf{A}^*)^{-1} + (1/\Delta t)\,(\mathbf{A}^*)^{-2}\,(\mathbf{A} - \mathbf{I})]\,\mathbf{B}^*$ is the $2n \times r$ discrete-time friction loading matrix of the current time step, $\mathbf{E}_0 = [(\mathbf{A}^*)^{-1}\,\mathbf{A} + (1/\Delta t)\,(\mathbf{A}^*)^{-2}\,(\mathbf{I} - \mathbf{A})]\,\mathbf{E}^*$ is the $2n \times q$ discrete-time external loading matrix of the previous time step, and $\mathbf{E}_1 = [-(\mathbf{A}^*)^{-1} + (1/\Delta t)(\mathbf{A}^*)^{-2}\,(\mathbf{A} - \mathbf{I})]\,\mathbf{E}^*$ is the $2n \times q$ discrete-time external loading matrix of the current time step.

The non-sliding conditions for each individual bearing are

$$|F_i[k]| < \mu_i W_i \tag{6a}$$

and

$$\dot{u}_i[k] = 0 \tag{6b}$$

whereas the sliding conditions for the bearing are

$$F_i[k] = \mu_i W_i \operatorname{sgn}(\dot{u}_i[k]) \tag{7a}$$

and

$$\dot{u}_i[k] \neq 0 \tag{7b}$$

where $F_i$ is the $i$th component of the friction force vector $\mathbf{F}[k]$, $\mu_i$ is the frictional coefficient of the $i$th sliding bearing, $W_i$ is the load carried by the $i$th sliding bearing, $\dot{u}_i$ is the relative velocity between the sliding interface of the $i$th sliding bearing, and sgn is the signum function.

*Modified shear-balance procedure*

Note that in Equation (5) the friction force $\mathbf{F}[k]$ of the current time instant is dependent on the motion conditions which, however, is not known as a priori. Therefore, the solution cannot be obtained directly through simple recursive calculations. Instead of using an iterative corrective pseudo-force procedure as commonly considered for non-linear dynamic analysis, a procedure based on the concept of shear balance at the sliding interface is proposed [9].

The friction mechanisms stated in Equations (6) and (7) suggests that the shear force and the sliding velocity of the bearing are indicators of the motion conditions. During the sliding phase, the friction force is known as defined by Equation (7a), but the sliding velocity remains unknown

 

as stated by Equation (7b). During the non-sliding phase, the friction force or equivalently the bearing shear, remains undetermined as indicated by Equation (6a), however, with the condition of zero sliding velocity instead (Equation (6b)). Therefore, either the friction force or the sliding velocity is known, depending on the motion condition. With this additional condition, the base shear $\mathbf{F}[k]$ at time instant $k$ can be determined, and the responses of the system can in turn be solved. This forms the rationale of the proposed shear-balance procedure.

The key step of the proposed Shear-Balance Procedure numerical scheme is that, at each time step, the analysis starts by assuming a non-sliding condition. This implies

$$\mathbf{y}[k] = \mathbf{D}\mathbf{z}[k] = \mathbf{0} \tag{8}$$

where $\mathbf{y}[k]$ is the $r \times 1$ bearing velocity vector, and $\mathbf{D} = [\mathbf{0}, \mathbf{B}^{\mathrm{T}}]$ is the $r \times 2n$ location matrix of the bearing velocity.

Substitution of Equation (5) for $\mathbf{z}[k]$ into Equation (8), the bearing shear $\mathbf{F}[k]$ that would block the system from sliding is predicted as

$$\bar{\mathbf{F}}[k] = -(\mathbf{D}\mathbf{B}_1)^{-1}\mathbf{D}(\mathbf{A}\mathbf{z}[k-1] + \mathbf{E}_0\mathbf{w}[k-1] + \mathbf{E}_1\mathbf{w}[k] + \mathbf{B}_0\mathbf{F}[k-1]) \tag{9}$$

According to the friction law, however, the resulted shear forces are always less than the maximum friction force of the corresponding bearing interface during a non-sliding phase. Defining $\bar{F}_i[k]$ as the $i$th component of $\bar{\mathbf{F}}[k]$, which corresponds to the friction force of the $i$th bearing, the possible motion conditions are:

(A) All the bearing shear forces are less than the corresponding maximum friction forces, i.e.

$$|\bar{F}_i[k] < \mu_i W_i \quad \forall i = 1, \ldots, r \tag{10}$$

This agrees with the non-sliding assumption made first in the analysis. With the friction force vector $\mathbf{F}[k] = \bar{\mathbf{F}}[k]$ so determined, the response $\mathbf{z}[k]$ of the dynamic system are then obtained explicitly from Equation (5).

(B) All the bearing shear forces are greater than or equal to the corresponding maximum friction forces, i..e

$$|\bar{F}_i[k]| \geqslant \mu_i W_i \quad \forall i = 1, \ldots, r \tag{11}$$

This obviously violates the presumed non-sliding condition according to the friction mechanism, and, the whole system should be in a sliding phase rather. Accordingly, the shear forces of all the bearing should be adjusted by

$$F_i[k] = \mu_i W_i \operatorname{sgn}(\bar{F}_i[k]) \quad \forall i = 1, \ldots, r \tag{12}$$

With the friction force vector $\mathbf{F}[k]$ so determined, the response $\mathbf{z}[k]$ of the sliding structure are then obtained explicitly from Equation (5).

(C) There are $p$ bearing shears ($p < r$) of the estimated shear force vector $\bar{\mathbf{F}}[k]$ exceeding their corresponding maximum friction forces. This also violates the assumed condition that all the bearings are in a non-sliding condition. Rearranging the estimated shear force vector to be

$$\bar{\mathbf{F}}^*[k] = \begin{bmatrix} \bar{\mathbf{F}}_1^*[k] \\ \bar{\mathbf{F}}_2^*[k] \end{bmatrix} = \mathbf{T}\bar{\mathbf{F}}[k] \tag{13}$$

where $\bar{\mathbf{F}}_1^*[k]$ is the $(r-p) \times 1$ shear force vector of the non-sliding bearings whose components $\bar{F}_{1j}^*$ satisfy the assumption, that is, $|\bar{F}_{1j}^*| < \mu_j W_j$, $\forall j = 1, \ldots, r-p$. $\bar{\mathbf{F}}_2^*[k]$ is the $p \times 1$ shear force

 

vector of the sliding bearings whose components $\bar{F}^*_{2j}$ violate the assumption, that is, $|\bar{F}^*_{2j}| \geqslant \mu_j W_j$, $\forall j = 1, \ldots, p$, and $\mathbf{T}$ is the $r \times r$ transformation matrix that defines the linear relationship between $\bar{\mathbf{F}}[k]$ and $\bar{\mathbf{F}}^*[k]$.

Using the same transformation matrix $\mathbf{T}$, the bearing velocity vector $\mathbf{y}[k]$ can be easily reshuffled as

$$\mathbf{y}^*[k] = \mathbf{P}\mathbf{F}^*[k] + \mathbf{Q}^*[k] \tag{14}$$

where

$$\mathbf{y}^*[k] = \mathbf{T}\mathbf{y}[k] = \begin{pmatrix} \mathbf{y}^*_1[k] \\ \mathbf{y}^*_2[k] \end{pmatrix} \tag{15}$$

$$\mathbf{F}^*[k] = \mathbf{T}\mathbf{F}[k] = \begin{pmatrix} \mathbf{F}^*_1[k] \\ \mathbf{F}^*_2[k] \end{pmatrix} \tag{16}$$

$$\begin{aligned} \mathbf{Q}^*[k] &= \mathbf{T}(\mathbf{D}\mathbf{A}\mathbf{z}[k-1] + \mathbf{D}\mathbf{B}_0\mathbf{F}[k-1] + \mathbf{D}\mathbf{E}_0\mathbf{w}[k-1] + \mathbf{D}\mathbf{E}_1\mathbf{w}[k]) \\ &= \begin{pmatrix} \mathbf{Q}^*_1[k] \\ \mathbf{Q}^*_2[k] \end{pmatrix} \end{aligned} \tag{17}$$

$$\mathbf{P} = \mathbf{T}\mathbf{D}\mathbf{B}_1\mathbf{T}^{-1} = \begin{bmatrix} \mathbf{P}_{11} & \mathbf{P}_{12} \\ \mathbf{P}_{21} & \mathbf{P}_{22} \end{bmatrix} \tag{18}$$

In the above equations, the transformed vectors with subscript 1 correspond to the non-sliding bearings while those with subscript 2 correspond to the sliding bearings. For the bearing in a non-sliding mode, their sliding velocities are null, implying

$$\mathbf{y}^*_1[k] = \mathbf{0} \tag{19}$$

whereas for bearings in the sliding mode, each component of the transformed friction force vector $\mathbf{F}^*_2[k]$ should be adjusted as

$$F^*_{2j}[k] = \mu_j W_j \operatorname{sgn}(F^*_{2j}[k]),\ j = 1, \ldots, p \tag{20}$$

From Equation (14), (19) and (20), the shear forces of the non-sliding bearings are calculated as

$$\mathbf{F}^*_1[k] = -\mathbf{P}^{-1}_{11}(\mathbf{P}_{12}\mathbf{F}^*_2[k] + \mathbf{Q}^*_1[k]) \tag{21}$$

In accordance with the non-sliding condition, magnitudes of the components $F^*_{1j}$'s of $\mathbf{F}^*_1$ should be no more than their corresponding maximum friction forces, $\mu_j W_j$. That is

$$|\bar{F}^*_{1j}| \leqslant \mu_j W_j, \quad \forall j \tag{22}$$

However, if $|\bar{F}^*_{1j}| \geqslant \mu_j W_j$, for any $j$, further iteration is required. Let $\bar{\mathbf{F}}[k] = \mathbf{T}^{-1}\mathbf{F}^*[k]$ and go through the previous procedures to check the motion condition until Equation (22) is satisfied. The friction force vector in the original co-ordinate is then determined by

$$\mathbf{F}[k] = \mathbf{T}^{-1}\mathbf{F}^*[k] \tag{23}$$

With the friction force vector so determined, the structural response of the system with hybrid supporting conditions can then be solved explicitly from Equation (5). Flow chart for the solution algorithm is illustrated in Figure 1.

 

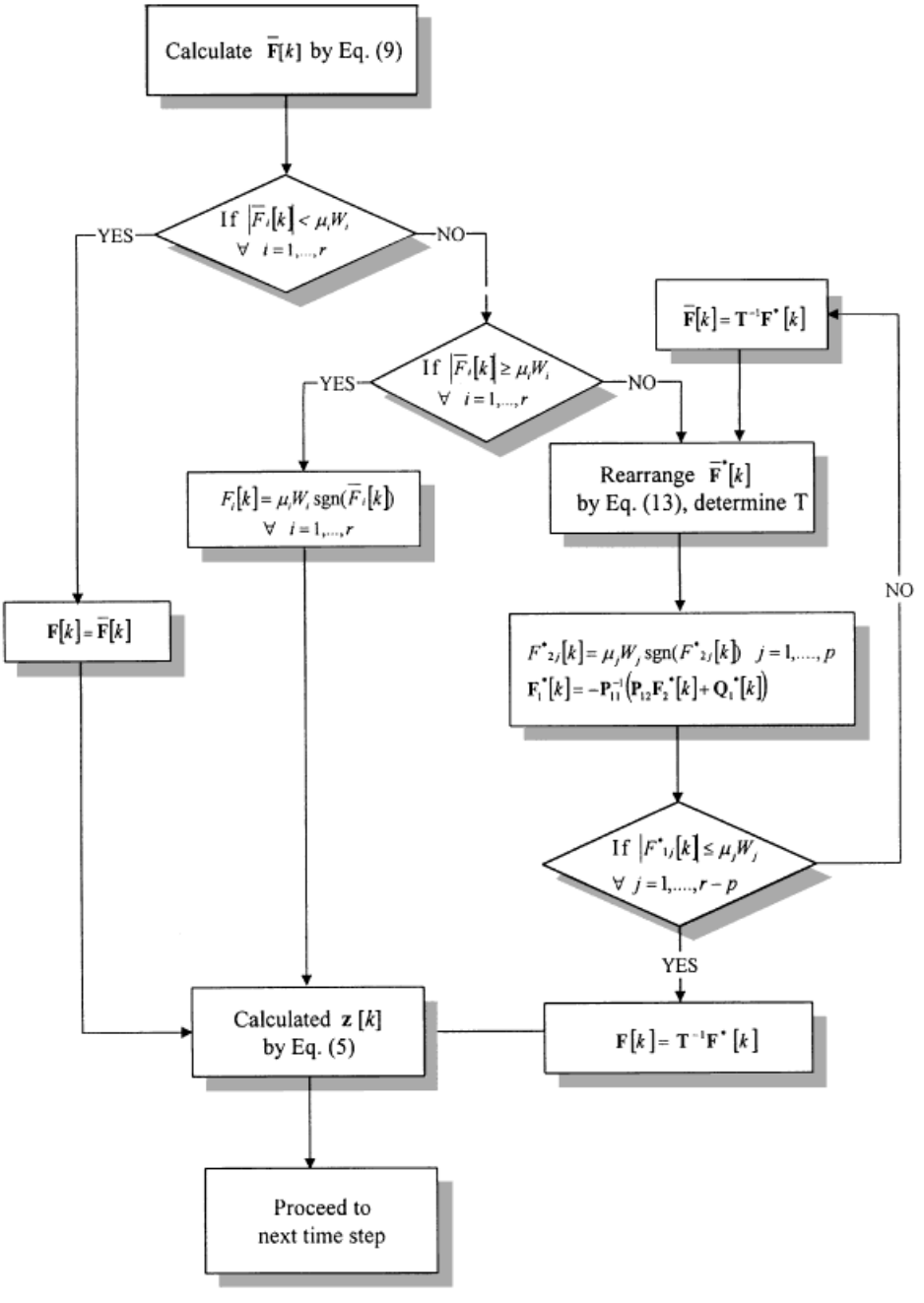


Figure 1. Flow chart for the proposed numerical algorithm.

 

The advantages of this proposed algorithm over the existing methods [9–12] are

(a) It allows for a more systematic analysis with a unified governing equation considered for both sliding and non-sliding modes.
(b) It requires less computational efforts with a constant and comparatively larger integration interval considered throughout the analysis.
(c) The friction force vector is obtained through simple matrix algebraic analysis satisfying equilibrium of shear forces and compatibility of motion conditions at the sliding interfaces.
(d) It is adaptive in dealing with systems with unsynchronized multiple isolation bearings.

## NUMERICAL EXAMPLES

*Example 1: Seismic isolation of a two-storey building erected on a stepped foundation*

Many hillside structures are built in accommodation with the slope, which results in elevation differences between the column footings, as in the two-storey house illustrated in Figure 2(a).

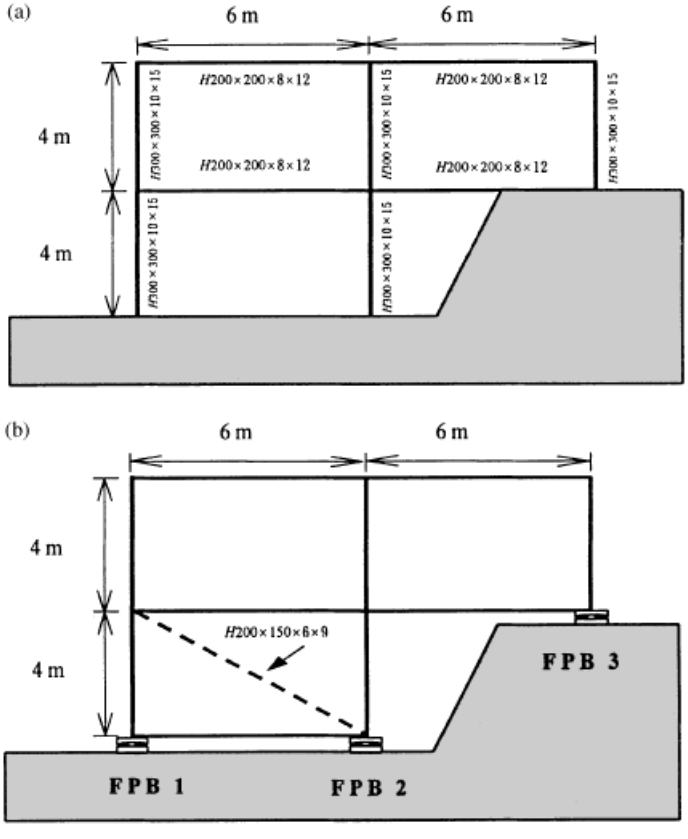


Figure 2. (a) Building on a stepped foundation without isolation, (b) building on a stepped foundation with isolation.

 

Owing to geometric asymmetry in elevation, this type of structure is vulnerable as it takes unevenly distributed column shears during earthquakes. If such a building is to be isolated with friction pendulum bearings against earthquakes, as shown in Figure 2(b), part of the isolation level is elevated. As a consequence, each of the sliding bearings implemented underneath the columns behaves independently due to structural asymmetry. Therefore, the design and the dynamic analysis of the isolated stepped-structures differ somewhat from the common practice. It is noted that, when isolated, the lower storey of the house is braced so as to avoid an unfavourable soft first storey configuration. Dimensions of the structural members are indicated in Figures 2(a) and (b). The fundamental natural frequency of the building before isolation is 2.23 Hz. The radius of curvature of the friction pendulum bearing is chosen to be 1.0 m so that the fundmental period of the isolated structure is shifted to approximately 2 s during sliding. Natural frequencies of the first five modes of the structure, with and without isolation, are summarized in Table I. Coulomb's model is considered for the friction mechanism of the sliding bearings with the frictional coefficient $\mu = 10$ per cent assumed. Material properties of the structural members considered are: Young's modulus $= 210 \times 10^9$ N/m$^2$, density $= 7.8$ t/m$^3$ and unit mass of slab $= 3.18$ t/m. The 1940 El Centro earthquake is used as input. The proposed numerical scheme is adopted for the dynamic analysis of this typical multiple-support sliding structure. Besides, a constant integration time interval $\Delta t = 0.01$ s is used throughout the analysis.

Effectiveness of seismic isolation for the stepped structure is examined by comparing the structural responses with those obtained without isolation. Simulation results are summarized in Table II. After isolation, the maximum storey drift of the first floor is reduced by 44 per cent, and the second floor by 74 per cent; the maximum storey shear of the first floor is reduced by 27 per cent, and the second floor by 80 per cent; the maximum acceleration of the first floor is reduced by 37 per cent, and the second floor by 74 per cent. The reason for a more pronounced reduction of the dynamic responses in the second floor is that, most of the earthquake forces are resisted by the upper level of the stepped structure if not isolated, whereas the earthquake forces are evenly distributed over the floors when isolated. Configuration of the peak floor displacement relative to the fixed base is illustrated in Figure 3. It is evident that significant reduction of the floor displacement of the isolated structure has been achieved with the allowance of base displacement as a tradeoff. The maximum sliding displacements of the friction pendulum bearings are 3.13, 3.14 and 3.26 cm, respectively, for FPB1, FPB2 and FPB3. The displacement responses of the bearings shown in Figure 4 are similar but not identical. It is interesting to note that small oscillations are observed for FPB3 at the upper level when the other bearings at the lower level are stuck, confirming the necessity of modeling the bearings independently in the analysis. Moreover, hysteresis of the bearing frictions shown in Figure 5 reflect precisely the Coulomb's frictional mechanism considered.

Table I. Natural frequencies of the building in Example 1.

| Structural type / Mode | | Fixed | Isolated |
|---|---|---|---|
| Natural frequeny (Hz) | 1 | 2.23 | 0.48 |
| | 2 | 14.29 | 2.88 |
| | 3 | 58.66 | 11.74 |
| | 4 | 88.03 | 23.85 |
| | 5 | 102.50 | 26.03 |

 

Table II. Assessment of isolation effectiveness (Example 1).

| Max. response quantity* \ Structural type | Fixed | Isolated | Reduction (%) |
|---|---|---|---|
| $D_1/H_1$ (%) | 0.085 | 0.048 | 44 |
| $D_2/H_2$ (%) | 1.570 | 0.405 | 74 |
| $S_1/W$ (%) | 22.8 | 16.7 | 27 |
| $S_2/W$ (%) | 65.4 | 13.1 | 80 |
| $ACC_1$ (g) | 0.67 | 0.42 | 37 |
| $ACC_2$ (g) | 1.29 | 0.34 | 74 |
| $DB_1$ (cm) | — | 3.13 | — |
| $DB_2$ (cm) | — | 3.14 | — |
| $DB_3$ (cm) | — | 3.26 | — |

* $D_1/H_1$ = storeydrift ratio of first floor (normalized with respect to storey height $H_1$);
$D_2/H_2$ = storeydrift ratio of second floor (normalized with respect to storey height $H_2$);
$S_1/H_1$ = storey shear of first floor (normalized with respect to structure's weight $W$);
$S_2/W$ = storey shear of second floor (normalized with respect to structure's weight $W$);
$ACC_1$ = acceleration of first floor;
$ACC_2$ = acceleration of second floor;
$DB_1$ = sliding displacement of FPB 1;
$DB_2$ = sliding displacement of FPB 2;
$DB_3$ = sliding displacement of FPB 3.

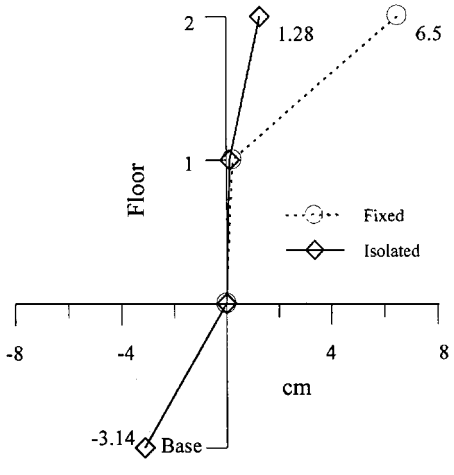


Figure 3. Peak floor displacements relative to fixed base (Example 1).

 

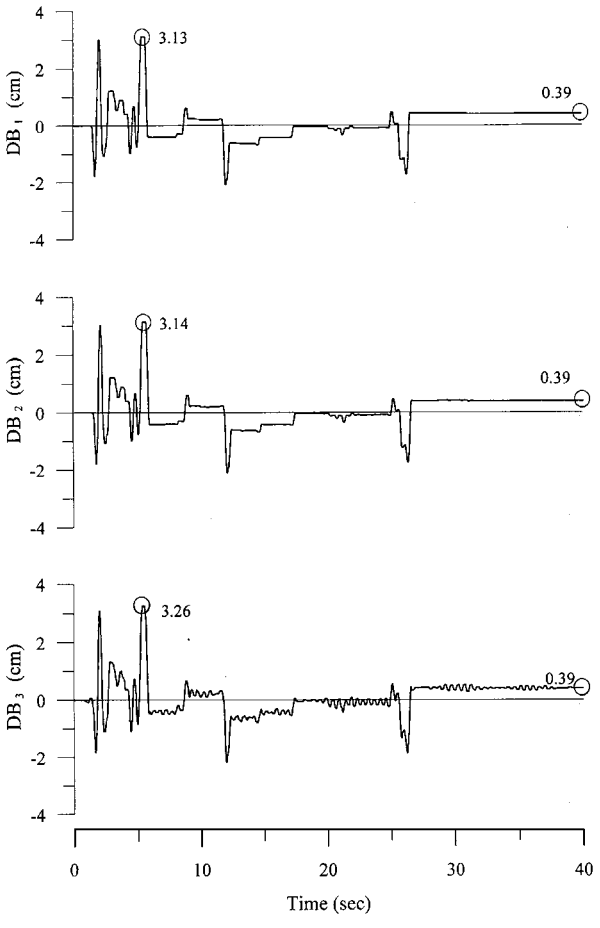


Figure 4. Sliding displacement of friction pendulum bearings (Example 1).

*Example 2: Seismic isolation of a continuous bridge*

A common three-span continuous bridge with hinge-type supports on the interior piers and roller-type supports on the exterior piers (abutments) is illustrated in Figure 6(a). Damage of the bridge structures due to earthquakes occurs occasionally in the piers, which may in turn result in collapse of the bridge spans. With the piers isolated from the bridge superstructure, the bridge and the piers vibrate independently during earthquakes so that the interactions between them are minimized. Replacing the supporting bearings by friction pendulum bearings for seismic isolation constitutes another sliding structure with unsynchronized support motion (Figure 6(b)). Independence of the bearing behaviours during earthquakes due to structural asymmetry is taken into account in the analytical model. The radius of curvature of the friction pendulum bearing is chosen to be 1.0 m so that the fundamental period of the isolated bridge is approximately 2 s during sliding. The frictional coefficient of the sliding bearings is assumed to be 10 per cent.

 

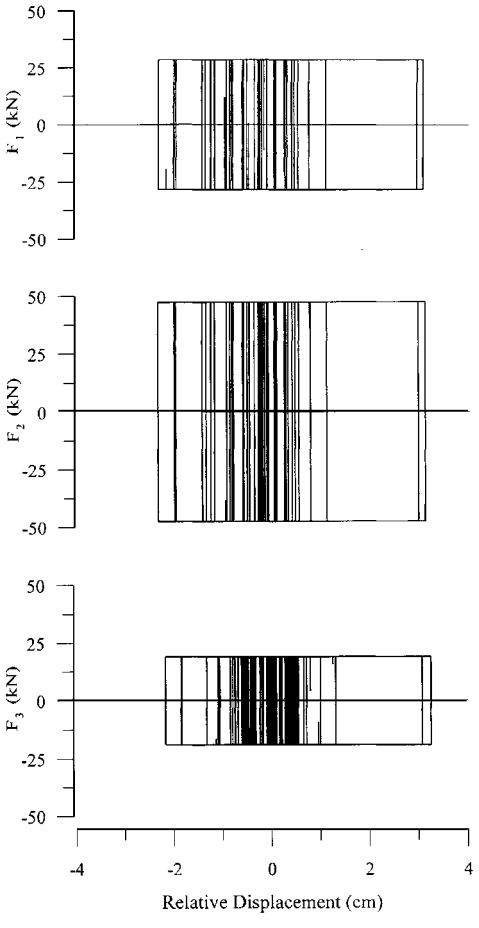


Figure 5. Hysteresis of Bearing Friction (Example 1).

Member properties of the bridge considered in the analysis are summarized in Table III. The 1940 El Centro earthquake is used as input and a constant integration time interval $\Delta t = 0.01$ s is used throughout the analysis.

Effectiveness of seismic isolation on bridge structures can best be assessed by examining the shears and moments at the piers' footings. As indicated from Table IV, beyond 80 per cent of peak reductions of the base shears at the interior piers (VP1, VP2) have been achieved when the bridge is isolated. Meanwhile, equivalent degrees of peak reduction of the moments at the interior piers (MP1, MP2) have been obtained, and so have the peak displacements at the top of the piers (DP1, DP2). Besides, peak displacement of the bridge superstructure (DS) is reduced by 43 per cent. Both reductions in the forces of the substructure and the displacements of the superstructure are achieved simultaneously. This might contradict to one's intuition that displacements of an isolated structure will be excessive. On the other hand, the base shears (VA1, VA2) and the base

 

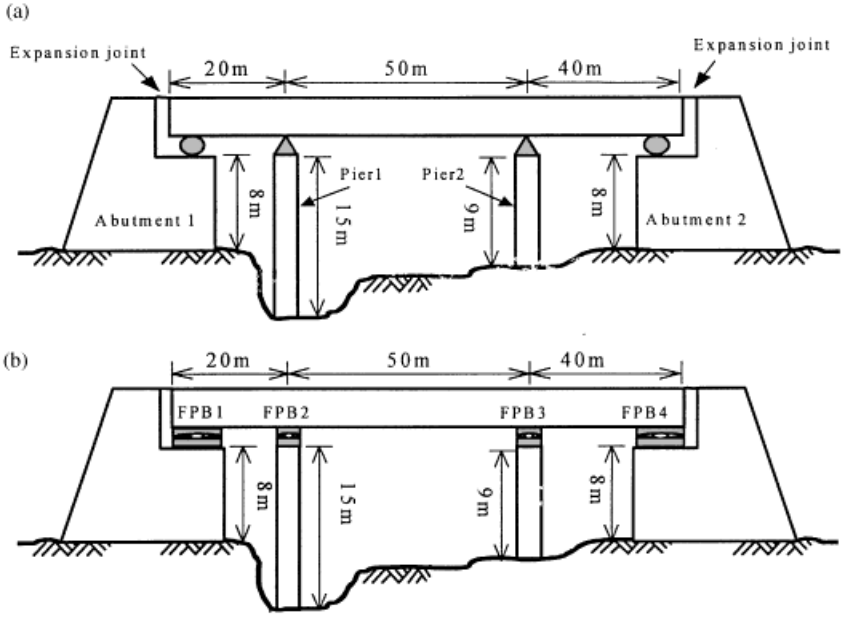


Figure 6. (a) Conventional continuous bridge (Example 2), (b) continuous bridge with seismic isolation (Example 2).

Table III. Bridge member properties (Example 2).

| | Superstructure | Pier | Abutment |
|---|---|---|---|
| Area ($m^2$) | 1.538 | 4.5 | 15 |
| Moment of inertia ($m^4$) | 3.7 | 0.84 | 2.81 |
| Young's modulus ($N/m^2$) | $2.04 \times 10^{11}$ | $2.05 \times 10^{10}$ | $2.05 \times 10^{10}$ |
| Density ($t/m^3$) | 7.8 | 2.4 | 2.4 |

moments (MA1, MA2) of the abutments are more or less increased when the bridge is isolated. The fact is that, with the conventional design, nearly 90 per cent of the earthquake forces are resisted by the piers on which the hinge-type bearings are implemented. This may not be judicious arrangement since, intrinsically stiffer, the abutments normally possess higher loading capacity than the piers. Therefore, it is not harmful to the bridge at all if the abutments share more loading during earthquakes. Actually, when the bridge is isolated, the overall earthquake forces to be carried by the substructure are not only remarkably reduced (70 per cent for the base shear and 67 per cent for the moment) but also fairly distributed between the piers and the abutments. Seismic isolation permits a more rational and effective earthquake-resistant mechanism. The sliding displacements of the bearings shown in Figure 7 are similar but not identical, confirming the

 

Table IV. Effectiveness assessment of seismic isolation (Example 2).

| Max. response quantity* \ Structural type | Conventional | Isolated | Reduction (%) |
|---|---|---|---|
| VP1 (kN) | 11402 | 2335 | 80 |
| VP2 (kN) | 19161 | 2438 | 87 |
| VA1 (kN) | 1912 | 2578 | − 35 |
| VA2 (kN) | 2758 | 2809 | − 2 |
| Sum. of shear | 35233 | 10160 | 70 |
| MP1 (kN m) | 34206 | 7784 | 77 |
| MP2 (kN m) | 57482 | 8126 | 86 |
| MA1 (kN m) | 5097 | 8595 | − 69 |
| MA2 (kN m) | 7356 | 9363 | − 27 |
| Sum. of moment | 104141 | 33868 | 67 |
| DP1 (cm) | 9.06 | 1.54 | 83 |
| DP2 (cm) | 9.03 | 1.59 | 82 |
| DA1 (cm) | 0.20 | 0.54 | − 170 |
| DA2 (cm) | 0.29 | 0.58 | − 100 |
| DS (cm) | 9.06 | 5.16 | 43 |

VP1 = shear of pier 1;
VP2 = shear of pier 2;
VA1 = shear of abutment 1;
VA2 = shear of abutment 2;
MP1 = moment of pier 1;
MP2 = moment of pier 2;
MA1 = moment of abutment 1;
MA2 = moment of abutment 2;
DP1 = displacement of pier 1;
DP2 = displacement of pier 2;
DA1 = displacement of abutment 1;
DA1 = displacement of abutment 1;
DA2 = displacement of abutment 2;
DS = displacement of superstructure;

necessity to model the bearings independently. The maximum sliding displacement of all occurs on FPB1 to be 4.99 cm, which is well within the tolerance of the expansion joints for bridges. Again in this example, the hysteresis of the bearing frictions shown in Figure 8 reflect precisely the Coulomb's frictional mechanism considered.

## CONCLUSIONS

Researches or engineering practice on base isolation up-to-date are mostly in regard of structures built on contour foundations. In order to simplify the analysis, synchronization of the kinematics of all the isolation bearings is often granted. However, synchronization of the motions of the isolation bearings at discretion may lead to inaccurate prediction of structural responses. Stepped

 

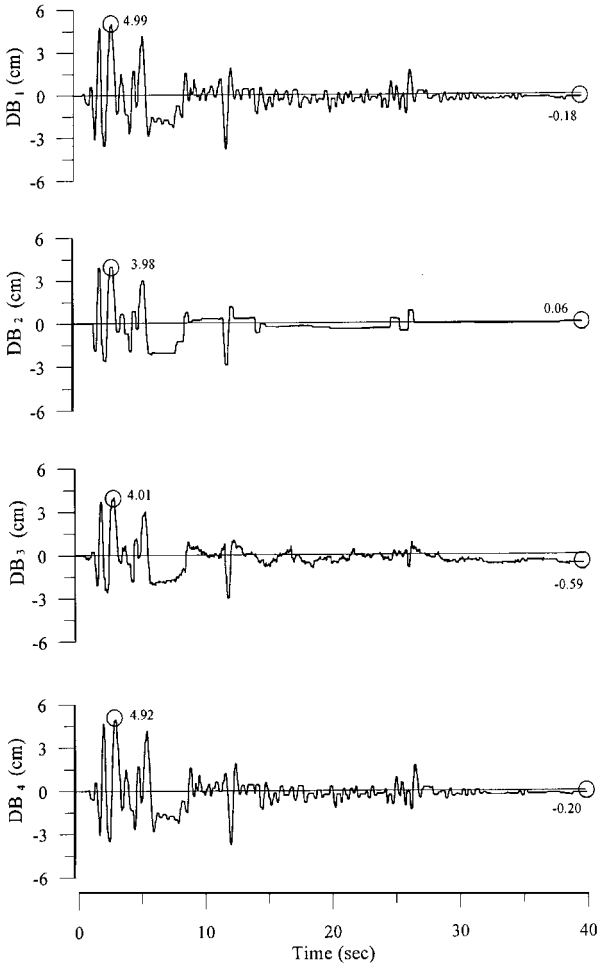


Figure 7. Sliding displacement of friction pendulum bearings (Example 2).

structures or continuous bridges with seismic isolation are notable examples where unsynchronized bearing motions are expected. Such problems, however, cannot be solved directly by the existing numerical procedures developed for sliding systems. In this paper, an innovative and systematic numerical procedure based on equilibrium of shears and compatability of the motion conditions at the sliding interfaces has been developed for dynamic analysis of sliding structures with unsynchronized support motions. According to the proposed scheme, a unified motion equation can be adapted for both the non-sliding and sliding phases of the system. The responses of the sliding structure are obtained recursively from the discrete-time version of the motion equation with constant integration time step even during the transitions between the non-sliding and sliding phases. Therefore, both accuracy and efficiency in the dynamic analysis of the highly non-linear system can be achieved. Feasibility of using friction pendulum bearings for seismic

 

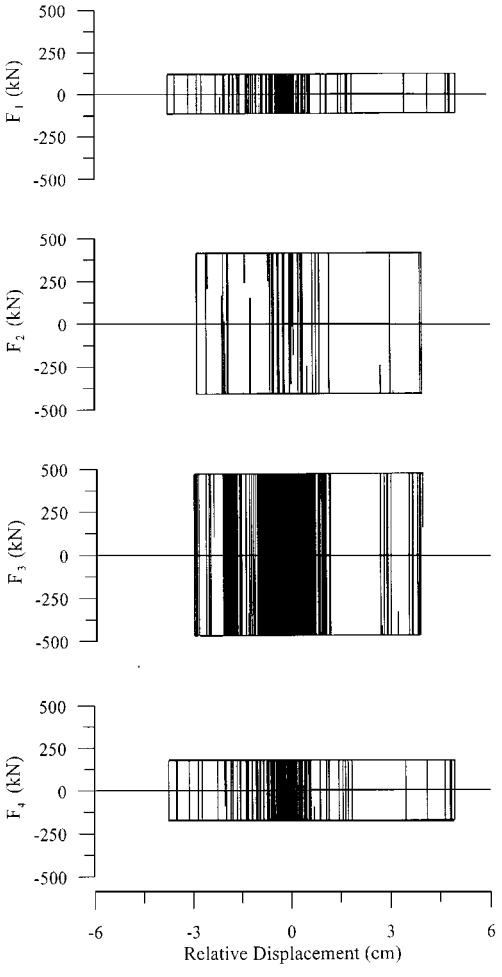


Figure 8. Hysteresis of bearing friction (Example 2).

isolation of both a stepped structure and a continuous bridge has been investigated under 1940 El Centro earthquakes. In the case of the stepped structure, simulation results indicate that significant reduction of the floor displacements, accelerations as well as the storey shears of the isolated structure can be obtained, with acceptable bearing displacements. In the case of the isolated continuous bridge, the overall earthquake forces to be carried by the substructure have shown to be remarkably reduced and fairly distributed between the piers and the abutments. Effectiveness of friction pendulum bearings on earthquake protection of stepped structures as well as continuous bridges has been assured. Moreover, evident unsynchronized sliding motions of the friction bearings have been observed in both examples, which confirms the necessity to deal with the bearings independently in the analysis.

 

ACKNOWLEDGEMENTS

This research is sponsored by the National Science Council of the Republic of China under Grant no. NSC 87-2621-P-009-002. The authors would like to thank Dr L. L. Chung, National Center for Research on Earthquake Engineering, Taiwan, for his valuable discussions.

REFERENCES

1. Buckle IG, Mayes RL. Seismic isolation history: application and performance — a world review. *Earthquake Spectra* 1990; **6**:161–201.
2. Zayas V, Low SS, Mahin SA. The FPS earthquake resisting system, experimental report. *Report No. UCB/EERC-87/01*, Earthquake Engineering Research Center, University of California, Berkeley, CA, June 1987.
3. Kawamura S, Kitazawa K, Hisano M, Nagashima I. Study of a sliding-type base isolation system—system composition and element properties. *Proceedings of the 9th WCEE*, Tokyo-Kyoto, vol V, 1998; 735–740.
4. Constantinou MC, Tsopelas P, Kim Y-S, Okamoto S. NCEER-Taisei corporation research program on sliding seismic isolation systems for bridges: experimental and analytical study of a friction pendulum system (FPS). *Technical Report NCEER-93-0020*, NCEER, SUNNY/Buffalo, NY, November, 1993.
5. Mokha AS, Constantinou MC, Reinhorn AM. Teflon bearing in base isolation. I: testing: *J. Struct. Engng*, ASCE 1990; **116**(2):438–454.
6. Mokha AS, Constantinou MC, Reinhorn AM. Teflon bearing in base isolation. II: Modeling. *J. Struct. Engng*, ASCE 1990; **116**(2):455–474.
7. Westermo B, Udwadia F. 'Periodic response of a sliding oscillator system to harmonic excitation', *Earthquake Engng Struct. Dyn.* 1983; **11**:135–146.
8. Mostaghel N, Hejazi M, Tanbakuchi J. Response of sliding structures to harmonic support motion. *Earthquake Engng Struct. Dyn.* 1983; **11**:355–366.
9. Mostaghel N, Tanbakuchi J. Response of sliding structures to earthquake support motion. *Earthquake Engng Struct. Dyn.* 1983; **11**:729–748.
10. Yang YB, Lee TY, Tsai IC. Response of multi-degree-of freedom structure with sliding supports. *Earthquake Engng Struct. Dyn.* 1990; **19**:739–752.
11. Lu LY, Yang YB. Dynamic response of equipment in structures with sliding support. *Earthquake Engng Struct. Dyn.* 1997; **26**:61–77.
12. Wang YP, Chung LL, Liao WH. Seismic response analysis of bridges isolated with friction pendulum bearings. *Earthquake Engng Struct. Dyn.* 1998; **27**:1069–1093.

 